Transactions of the **14th International Conference on Structural Mechanics in Reactor Technology** (SMiRT 14), Lyon, France, August 17-22, 1997 **LW/10**

Modelling of uniaxial and multiaxial ratchetting of stainless steel 316 SPH by a micromechanical approach

Pilvin P.[1], **Geyer P.**[2]
(1) Centre des Matériaux, ENSMP, France
(2) EDF, France

ABSTRACT : With experimental results on SS 316 SPH obtained at room temperature, the advantage of a polycristalline approach to study the cyclic behavior is shown. First, the constitutive equations of the model developed at the Centre des Matériaux (CdM) are described. Then the model predictive capability is studied through uniaxial and multiaxial tests with emphasis on ratchetting.

1. INTRODUCTION

Ratchetting is one of the most complex phenomena for cyclic loadings. It has been studied since more than fifteen years. Several constitutive equations based on a phenomenological approach have been proposed recently to improve the modelling of ratchetting. The weakness of this approach is its inductive feature : if a test exhibits a new material phenomenon, it is necessary to modify the model.

With experimental results on SS 316 SPH obtained at room temperature [1, 2], the advantage of a micromechanical approach to study the cyclic behavior is shown. First, the constitutive equations of the model developed at the Centre des Matériaux [3] are described. Then the model predictive capability is studied. Emphasis is put on material parameters identification with respect of the self-consistent scheme of the homogenization process.

2. THE POLYCRYSTALLINE MODEL USED

The polycrystalline model developed at CdM is described in this section. A number of proposals have been advanced in recent years for the modelling of the mechanical behaviour of metallic polycrystals with a micromechanical approach [4, 5]. This approach (one-site self-consistent scheme) provides a frame of reference for the proposed model with special attention to cyclic behaviour.

The heterogeneity of the representative volume element (RVE) of the material is introduced in the model, together with the representation of the elementary deformation mechanisms. A sound knowledge of the microstructure is then needed, and the main difficulty arising with this type of approach is the choice of the pertinent scale and of the critical mechanisms. In the specific case of polycrystalline metallic materials, a crude description is currently used. It follows that the dislocations cannot be directly represented and, for most of the classical

models, only the first heterogeneity level is considered : the grain. If the size and the shape of grains are virtually identical, all grains with the same crystallographic orientation are equivalent. Then it is possible to defined a "phase" with its orientation (Euler's angles) and its volume fraction (f_g). The size or the relative position of one grain with respect to the other are not taken into account (no size effect, no neighbourhood effect).

For a phase, the modelling of the inelastic deformation is generally restricted to the effect of crystallographic slip. The behaviour is related to the generalised Schmid law, which assumes that a slip system is active when its shear stress reaches a critical value. The description of the hardening is then introduced at this level, provided the value of this critical shear stress on each slip system depends on hardening variables. In the case of small strain and small rotation formalism, the plastic strain ε^p of a phase is obtained from the knowledge of the average shear strain Γ_s on each slip system :

$$\varepsilon^p = \sum_{s \in S} \mathbf{m}_s \Gamma_s \quad \text{with} \quad \mathbf{m}_s = \frac{1}{2} [\, \mathbf{n}_s \otimes \mathbf{l}_s + \mathbf{l}_s \otimes \mathbf{n}_s] \tag{1}$$

In the previous expression, $\mathbf{m}_s$ characterises the orientation of the slip system defined by the unit vector $\mathbf{n}_s$, normal to the slip plane, and the unit vector $\mathbf{l}_s$, giving the slip direction. The calculation of the resolved shear stress for the slip system can also be expressed as a function of the average stress in the phase σ, by means of the same tensor : $T_s = \sigma : \mathbf{m}_s$. The definition of the mechanical behaviour on the elementary level is completed by the evolution rules for internal variables. The formulation on this level is made in the framework of viscoplasticity. This choice allows one to directly compute the shear strain rate from the actual value of the stress and of the internal variables. Nevertheless, with suitable values of the viscosity coefficients (K and N), the global behaviour becomes time-insensitive. One of the specificity of the model is the introduction of hardening internal variables able to model the cyclic behaviour [6]. Two hardening variables are introduced for each mechanism. The latent hardening, which is correlated with overstrengthening associated with nonproportional loading, is modelled by an isotropic variable R_s and an interaction matrix H_{rs}. The kinematic hardening variable X_s accounts for the local heterogeneities inside the phase.

$$\dot{\Gamma}_s = \left[\mathrm{Max}\{0; \frac{F_s}{K}\}\right]^N \mathrm{Sign}(T_s - X_s) \quad ; \quad F_s = |T_s - X_s| - \tau_0 - R_s + \frac{1}{2}\frac{D}{C} X_s^2 \tag{2a}$$

$$X_s = C\,\alpha_s \quad ; \quad R_s = Q \sum_{r \in S} H_{rs}\, q_r \tag{2b}$$

$$\dot{\alpha}_s = \dot{\Gamma}_s - D\,\alpha_s |\dot{\Gamma}_s| \quad ; \quad \dot{q}_s = |\dot{\Gamma}_s| (1 - B\,q_s) \tag{2c}$$

We select only one parameter to define the interaction matrix (H_{rs}=1 if r=s, H_{rs}=H if r≠s). Hence, eight material constants, A_g = (K, N, τ_0, D, C, Q, B, H), are introduced to describe the transgranular viscoplastic behavior.

The final aspect of the polycrystalline model is the definition of the relations between the variables in each phase of the aggregate (σ, ε, ε^p) and the macroscopic variables (Σ, $\mathbf{E}$, $\mathbf{E}^p$). For simplicity, we assume that elasticity of each phase is isotropic (μ : Coulomb's modulus, ν : Poisson's ratio). In this case, the macroscopic plastic strain is the average of the local plastic strains and the macroscopic stress can be deduced from Hooke's law :

$$\mathbf{E}^p = \sum_{g\in G} f_g \varepsilon^p \quad ; \quad \Sigma = \sum_{g\in G} f_g \sigma = 2\mu \{ \mathbf{I} + \frac{\nu}{1-2\nu} \mathbf{1}\otimes\mathbf{1} \} (\mathbf{E} - \mathbf{E}^p) \tag{3}$$

The self-consistent approach is an appropriate tool for estimating the stress in each phase. To represent the interaction between the phase and the homogeneous equivalent medium (HEM), this approach computes the stress and the strain in a phase, the individual behaviour of which is known, as the result of a boundary value problem : an inclusion (the phase) in an infinite homogeneous matrix (the HEM) submitted to uniform boundary conditions. A rigourous treatment of this problem has been made by Hill for time independent plasticity [4], but the numerical treatment of the resulting implicit integral equation is not simple.

For elastoviscoplasticity, we used an approximate localisation rule and the self-consistent conditions (SCC) of the model are checked numerically. The localisation rule used in the model is given *a priori* under an explicit form (4). It involves a specific variable for each phase β^g to produce a non linear accommodation of the intergranular incompatibilities :

$$\sigma = \Sigma + \frac{2}{15}\frac{7-5\nu}{1-\nu}\mu \left\{ \mathbf{B} - \beta^g \right\} \quad \text{with} \quad \mathbf{B} = \sum_{g\in G} f_g \beta^g \tag{4}$$

The general form of the evolution law of this variable is given by :

$$\dot{\beta}^g = \dot{\varepsilon}^p - \mathbf{G}(\beta^g, \varepsilon^p, \mathbf{B}, \mathbf{E}^p) \| \dot{\varepsilon}^p \| \quad \text{with} \quad \| \dot{\varepsilon}^p \| = \sqrt{\frac{2}{3} \dot{\varepsilon}^p : \dot{\varepsilon}^p} \tag{5}$$

If the value of the function **G** is zero at origin, this form is compatible with the so-called Kröner's model [7] on the onset of plastic flow and we have to find the expression of the function **G** to satisfy as best as possible the SCC. It is suitable to introduce tuning parameters in this function. These parameters are not material constants but they are related to local behaviour. They have to be determined as explained in section 4. Within the frame of small strain, we used a linear expansion of the function **G** into a series about origin. Then, four parameters, $\mathbf{A}_\beta$ (Δ, δ, Φ, ω) are introduced and the evolution law of the variable is :

$$\dot{\beta}^g = \dot{\varepsilon}^p - \Delta\{ \beta^g - \delta \varepsilon^p + \Phi \mathbf{B} + \omega \mathbf{E}^p\} \| \dot{\varepsilon}^p \| \tag{6}$$

In previous works [3], the parameters Φ, ω of this equation equal zero. This additional feature is due to the introduction of the SCC in the identification method as explained in the next section.

4. IDENTIFICATION OF MATERIAL CONSTANTS

The set of parameters, $\mathbf{A} = (\mathbf{A}_g, \mathbf{A}_\beta)$, of the constitutive equations given previously are identified by a quantitative comparison of the experimental observations $\mathbf{Z}^{exp}$ and the modelled simulations of these experiments $\mathbf{Z}^{sim}$. This identification task is classically formulated with an optimization problem based on the cost function $\pounds(\mathbf{A})$ defined in (7) where the symbol $|\bullet|$ represents a norm on the space of the observable variables (strain, displacement, load, temperature, ...) and I_j the observation interval in the j^{th} test of the experimental data base ϑ [8].

$$\pounds(\mathbf{A}) = \sum_{j\in\vartheta} \int_{t\in Ij} | \mathbf{Z}^{exp}(t) - \mathbf{Z}^{sim}(\mathbf{A}, t) | \, dt \tag{7}$$

For the proposed model, the parameters A_β have to be determined with the SCC of the homogenization process. The identification method has therefore been modified to allow for these conditions. A penalty term is introduced in the cost function in order to constrain the optimization process. The self-consistency of the model is estimated by the comparison of the results of boundary value problems (each cell embedded in a "infinite" HEM) and the results of the model predictions with the same loading paths (homogeneous strain prescribed at the boundary). A finite element (FE) code is used to solve each boundary value problem, after which it is easy to calculate the average stress (resp. strain) in each phase denoted σ^{Ref} (resp. ε^{Ref}). With these results, the SCC are expressed by, for all loading paths :

$$\forall\, g\in G \quad ; \quad \forall\, t \quad ; \quad \sigma^{Ref} - \sigma^{\beta} = 0 \quad \text{and} \quad \varepsilon^{Ref} - \varepsilon^{\beta} = 0 \tag{8}$$

where the stress (resp. strain) in each phase predicted by the model are denoted σ^β (resp. ε^β). Then, the optimization problem used a penalty cost function defined by

$$\pounds_p(\mathbf{A}) = \pounds(\mathbf{A}) + \sum_{g\in G} \int \{ |\sigma^{Ref} - \sigma^{\beta}| + |\varepsilon^{Ref} - \varepsilon^{\beta}| \}\, dt \tag{9}$$

This approach have been used previously for two-phase single crystals [9] and two-phase polycrystals [10]. One drawback of this approach is due to the large amount of CPU time but it is necessary when the viscous effects are significant [11]. If the macroscopic behaviour is roughly isotropic and have weak rate dependant effects, it is possible to reduce this dificulty. In this case we used the so-called Berveiller-Zaoui's model [12] as a reference solution for radial monotonic loading paths to estimate the SCC without FE analysis. Then, at each iteration of the minimisation algorithm, we compute σ^{Ref} and ε^{Ref} with the localisation rule given by

$$\sigma = \Sigma + \frac{2}{15}\frac{7-5\nu}{1-\nu}\, \alpha(\Sigma, \mathbf{E}^p)\, \mu \left\{ \mathbf{E}^p - \varepsilon^p \right\} \quad \text{with} \quad \alpha^{-1} = 1 + \frac{3}{2}\mu \frac{\|\mathbf{E}^p\|}{J_2(\Sigma)} \tag{10}$$

FE analysis can also be used to check *a posteriori* the validity of the scale transition rule when the local behaviour is known. We illustrate this with a dummy FCC polycrystal (see Table 1 for material parameters with μ=68.7 GPa, ν=0.31 and N=25). For FCC polycrystals, the predominant deformation mechanism is the crystallographic slip on the twelve octahedral systems {111} <110>. The computations with the polycrystalline model are performed by using the orientation distribution function, taken under a discrete form. If the crystallographic texture is not very sharp, an isotropic distribution is chosen. It is made of 40 orientations ($\forall$ $g\in$ G; f_g=1/40). To estimate the parameters A_β (see Table 1), we compute the cost function with two numerical tests : a pure tensile test ($E_{33}(t) = \dot{\varepsilon}\, t$ with E_{33}^{max} = 2 % and $\dot{\varepsilon}$ = 2. 10^{-4} s^{-1}) and a pure shear test ($2E_{23}(t) = \dot{\varepsilon}\, t$ with E_{23}^{max} = 1 %). To check *a posteriori* the validility of these scale transition rules, we performed FE analysis under axisymmetric conditions with two specific orientations for the inclusion (soft phase : <001> // $\mathbf{e}_z$ and hard phase : <111> // $\mathbf{e}_z$). In each case, the matrix behaviour is defined by the the polycrystalline model and homogeneous strain is prescribed on the boundary : $\mathbf{E}(t) = E_{zz}(t) \left\{ \mathbf{e}_z\otimes\mathbf{e}_z - 1/2\, (\mathbf{e}_r\otimes\mathbf{e}_r + \mathbf{e}_\theta\otimes\mathbf{e}_\theta) \right\}$. Fig. 1 illustrates, for axial components of average strain and stress in the inclusion, the comparison between FE analysis and direct application of both scale transition rules on the RVE with the same loading path ($E_{zz}(t) = \dot{\varepsilon}\, t$ with E_{zz}^{Max} = 1 % and $\dot{\varepsilon}$ = 1. 10^{-4} s^{-1}). We may get a rough idea of the approximation of the self-consistent scheme for monotonic loading paths. Computations for cyclic and non proportional loading paths are in progress. As illustrated by isovalues of axial plastic strain (when E_{zz} = 1 %) in Fig. 2, we can see that mechanical fields are heterogenous near inclusion. These results differ from the Berveiller-Zaoui's approach in that they assume an uniform isotropic behaviour for the matrix [12]. His findings further suggest that an approximative matrix behaviour is adequate to solve the scale transition problem.

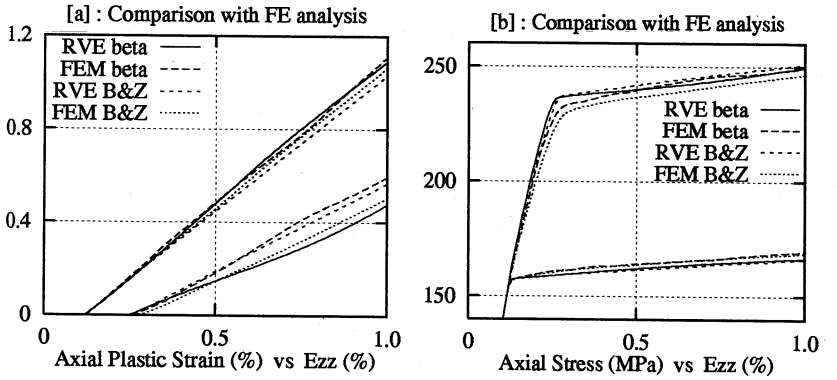

Figure 1: Validation of scale transition rules with FE analysis

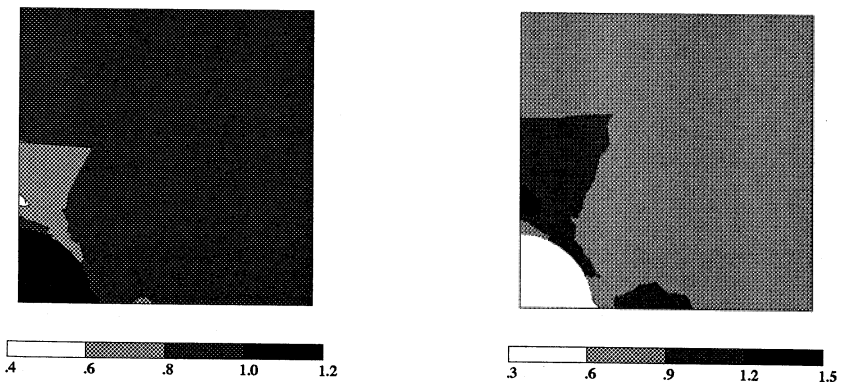

Figure 2: Isovalues of ε_{zz}^{p} (%) with B.&Z. localisation rule. Inclusion = soft phase (left), inclusion = hard phase (right)

4. APPLICATION TO THE 316 STAINLESS STEEL

Identification of material constants for a 316 stainless steel at 20 °C. The steel specimens are obtained from slabs taken from 30 mm thick sheets and hyperquenched from 1200°C. The microstructure is completely austenitic and the average size of the grains is 45 μm. The identification has been performed with an automatic procedure using the software SiDoLo [8]. For the identification uniaxial tension-compression tests under strain or stress control [1], biaxial constant pressure cyclic tension tests, biaxial constant tension cyclic torsion tests and triaxial constant pressure cyclic tension-torsion tests [2] have been used. In both cases different strain or stress amplitudes of loading have been used. Numerical values for the material parameters are presented in Table 1 with μ=68.7 GPa, ν=0.31 for elasticity constants. Because no specific tests for rate dependent effects are available, the viscous exponent is fixed to a classical value (N=25). Numerical results used to estimate the parameters A_β with the SCC are given in Fig. 3 for the tensile test (4 phases with different orientations are plotted). Comparison between experiments and model for monotonic tensile test ($\dot{\varepsilon}$= 1. 10^{-3} s^{-1}) and for low cycle fatigue tests with two amplitudes is given in Fig. 4a. Fig. 4b illustrates the same comparison for the cyclic hardening during a fatigue test ($\Delta\varepsilon = \pm 0.6$ %).

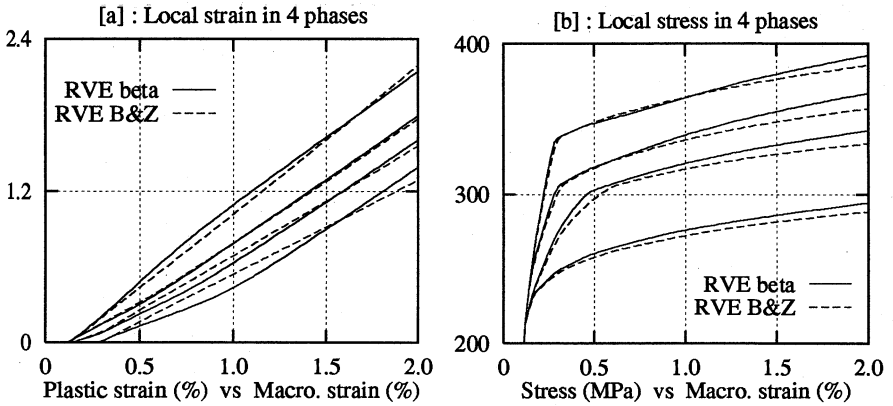

Figure 3: Comparison at phase level of both localisation rules for tensile test

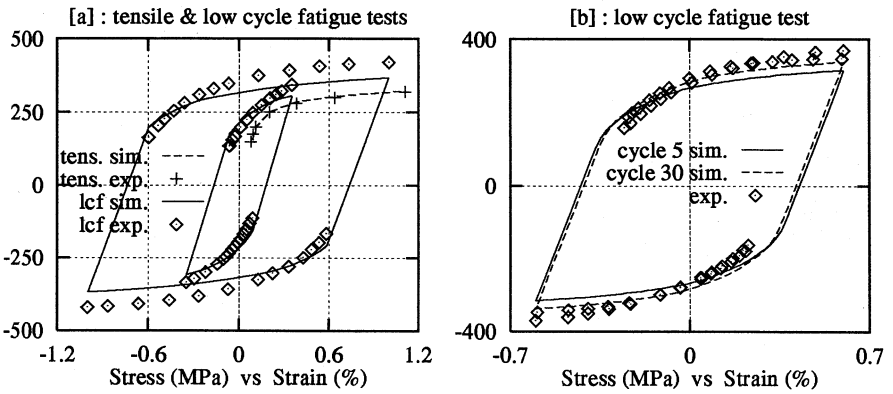

Figure 4: Classic tests : comparison between experiments and simulations

The uniaxial ratchetting behavior under stress control tests ($\sigma_{min} = \underline{\sigma}-\Delta\sigma/2$, $\sigma_{Max} = \underline{\sigma}+\Delta\sigma/2$) of the model is given in Fig. 5 {r1_1 ($\Delta\sigma/2$=50 MPa) : $\underline{\sigma}$=200 and 250 MPa; r1_3 ($\Delta\sigma/2$=245 MPa) : $\underline{\sigma}$=0 and 100 MPa; r1_4 ($\Delta\sigma/2$=180 MPa) : $\underline{\sigma}$=100 and 200 MPa; Test r1_5 ($\Delta\sigma/2$=120 MPa) : $\underline{\sigma}$=100 and 200 MPa}. Fig. 6a shows a comparison between model and biaxial ratchetting experiments {r2_1 (σ_{zz}=50 MPa) : $\Delta\varepsilon_{\theta z}$=±0.4 and ±0.52 %; r2_2 ($\sigma_{\theta\theta}$=50 MPa) : $\Delta\varepsilon_{zz}$=±0.4 and ±0.6 %} and the ratchetting behavior under triaxial constant pressure cyclic tension-torsion tests is given Fig. 6b (see Delobelle, 1995 for the loading paths). More details are given in the Fig. 7 for the first cycles of the biaxial ratchetting experiment labelled r2_1.

Material	Δ	δ	Φ	ω	τ_0	Q	B	C	D	K	H
dummy	505	0.189	0.112	0.125	70	0	/	2000	50	40	/
A 316L	480	0.183	0.122	0.112	74.4	3.73	3.76	2010	47.8	37.9	2.09

Table 1 : Coefficients of the polycrystalline model used for the simulations (units : MPa, s)

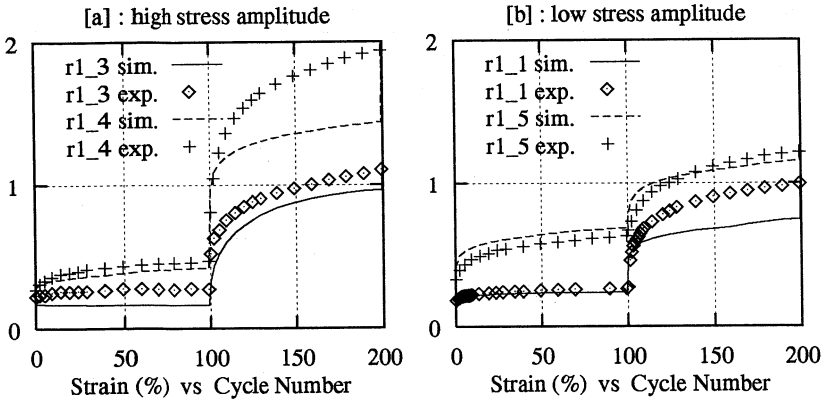

Figure 5: 1D ratchetting tests : Comparison between experiments and simulations

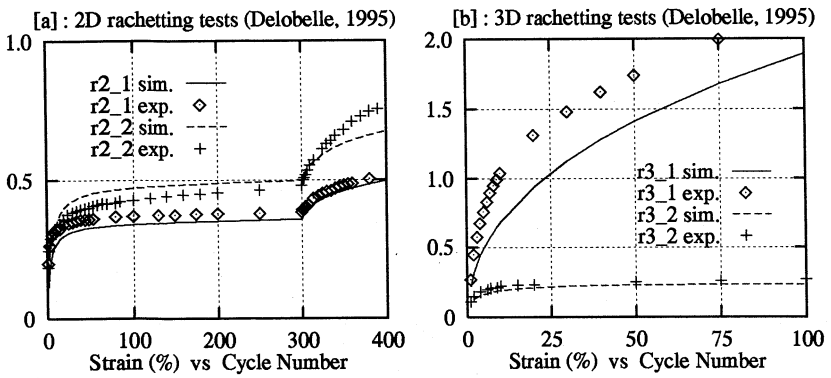

Figure 6: 2D & 3D ratchetting tests : Comparison between experiments and simulations

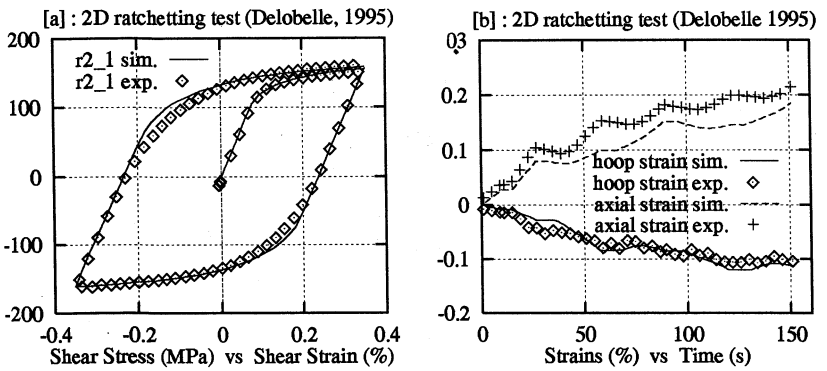

Figure 7: Comparison between experiment and simulation at the first cycles

5. CONCLUSIONS

The comparisons between the simulations and the experiments reported in this paper clearly show that, even using a simplified description of the microstructure, the polycrystalline approach have good modelling capabilities. In spite of the fact that the number of variables in these models is large, it is not a strong limitation for the use in structural computations problems [13].

REFERENCES

1. Engel, J.J. & G. Rousselier 1985. EdF report HT/PV D 599 MAT/T 43.

2. Delobelle, P., P. Robinet & L. Bocher 1995. Experimental study and phenomenological modelization of ratchet under uniaxial and biaxial loading on an austenitic stainless steel. *International Journal of Plasticity* 11:295-330

3. Pilvin, P. 1994. The contribution of micromechanical approaches to the modelling of the inelastic behaviour of polycrystals.
Proc. Int. Conf. on Biaxial/Multiaxial Fatigue: 31-46. Saint-Germain en Laye: ESIS/SF2M.

4. Hill, R. 1965. Continuum micro-mechanics of elastoplastic polycrystals.
Journal of the Mechanics and Physics of Solids 13: 89-101

5. Zaoui, A. 1985. *Homogenization Techniques for Composite Media.*
Lectures delivrered at the CISM (Udine), Springer-Verlag

6. Cailletaud, G. 1992. A micromechanical approach to inelastic behaviour of metals.
International Journal of Plasticity 8: 55-73

7. Kröner, E. 1961. Zur plastischen Veformung des Vielkristalls.
Acta Metallurgica 9: 155-161

8. Pilvin, P. 1988. Identification des paramètres de modèles de comportement.
Proc. MécaMat'88: 155-164. Besançon (France).

9. Forest, S. & P. Pilvin 1995. Modelling the cyclic behaviour of two-phase single crystal Nickel-base superalloys.
Proc. IUTAM Symp. on Micromechanics of Multiphase Materials: 51-58. Sèvres:Kluwer

10. Pilvin, P., X. Feaugas & M. Clavel 1995. A micro-macro structural approach of the cyclic behaviour of a two-phase alloy.
Proc. IUTAM Symp. on Micromechanics of Multiphase Materials: 51-58. Sèvres: Kluwer

11. Pilvin, P. 1997. Une approche inverse pour l'identification d'un modèle polycristallin élastoviscoplastique.
To be published in *Proc. of 3ème Colloque National en Calcul de Structures*. Giens (France)

12. Berveiller, M. & A. Zaoui 1979. An extension of the self-consistent scheme to plastically flowing polycrystals.
Journal of the Mechanics and Physics of Solids 26 : 325-344.

13. Vogel, C., E. Lorentz, P. Pilvin & S. Taheri 1997. A constitutive law using a ratchetting stress for description of progressive deformation and comparison with polycrystalline model.
This volume

Conception XEROX BUSINESS SERVICES
Achevé d'imprimer en Juillet 1997 par l'Imprimerie Bayeusaine, 14401 Bayeux - Dépôt légal : Juin 1997